AD-A064 790 SCIENCE APPLICATIONS INC MCLEAN VA F/G 4/1
THE EFFECT OF OCEAN THERMAL POWER PLANTS ON THE THERMODYNAMIC C--ETC(U)
SEP 77 R M CLANCY N00014-76-C-0610
UNCLASSIFIED SAI-78-665-W/A NL

| OF |
ADA
064790

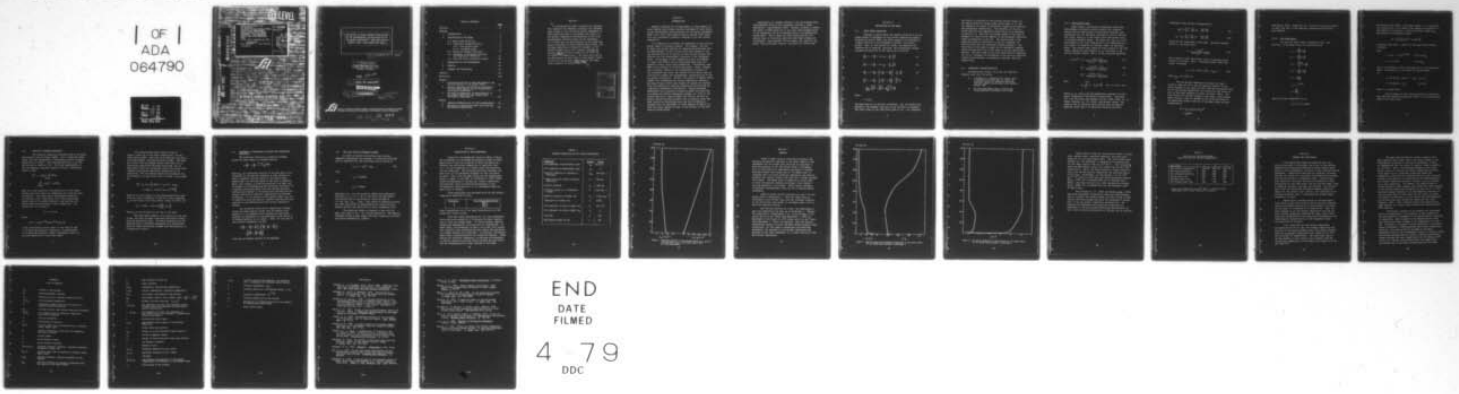

END
DATE
FILMED
4 79
DDC

LEVEL II

Science Applications, Inc.
SAI-78-665-WA.
THE EFFECT OF OCEAN THERMAL EPOWER PLANTS ON THE THERMODYNAMIC CHARACTERISTICS OF THE MARINE ATMOSPHERE: SOME PRELIMINARY RESULTS FROM A ONE-DIMENSIONAL MODEL.
1/4 in. thick, September 20, 1977

UNCLASSIFIED

Copy # (Rec'd)	Date	Copy # (Dest)	Date
1	12-16-77		

NRL 533027
Clancy, R.M.

N00014-76-C
0610

SCIENCE APPLICATIONS, INC.

(6) THE EFFECT OF OCEAN THERMAL POWER PLANTS ON THE THERMODYNAMIC CHARACTERISTICS OF THE MARINE ATMOSPHERE: SOME PRELIMINARY RESULTS FROM A ONE-DIMENSIONAL MODEL,

(15) N ~~0014~~-76-C-~~0620~~

(10) R. Michael Clancy
Fluid Mechanics Division
Science Applications, Inc.
McLean, Virginia

NRL 533,027

(14) SAI-78-665-WA

[redacted] FOR PUBLIC [redacted]
DISTRIBUTION UNLIMITED

(11) 20 Sep[redacted]77

(12) 31p.

TABLE OF CONTENTS

Abstract

A one-dimensional model consisting of conservation equations for momentum, moisture, and thermodynamic energy in the cloud-free marine atmosphere is constructed and used to investigate the effect of sea surface temperature perturbations on the local thermodynamic characteristics of the atmosphere. It is found that for perturbations in the range that would be produced by Ocean Thermal Power Plants, the average temperature and specific humidity in the marine boundary layer vary linearly with the sea surface temperature with slopes of 0.8 °C/°C and 0.6 g/kg/°C respectively. The total heat flux at the sea surface is also found to vary almost linearly with the sea surface temperature in the range with a slope of 31 cal/cm^2/day/°C.

Section 1

INTRODUCTION

Adequate planning for the deployment of large numbers of ocean thermal power plants requires knowledge of their effect on the thermodynamic characteristics of the marine atmosphere. OTPP's will alter these characteristics because their operation will necessarily produce a lowering of the sea surface temperature.

It is essential to estimate the magnitude of this environmental impact for several reasons. For example, the rate at which the thermal resource is regenerated downstream from an OTPP depends, in part, on the total heat balance at the sea surface which is a function of both the sea surface temperature and the thermodynamic structure of the atmosphere above. An estimate of this regeneration rate is necessary to insure that OTPP's are not positioned where they will adversely affect other plants downstream. Furthermore, many OTPP's will probably be located near shore. Hence, changes they ultimately induce in the thermodynamic structure of the atmosphere may affect the climate of the coastal zone by altering the dynamic and thermodynamic characteristics of the sea breeze circulation. Finally, the results of Shukla (1975) suggest that widespread sea surface temperature anomalies may significantly affect the climate of regions far removed from the anomalies by reducing evaporation and altering the large-scale atmospheric flow pattern. Shukla performed experiments with a general circulation model and found that an average sea surface temperature anomaly of $-1.5^{\circ}C$ in the Arabian Sea over a region roughly the size of the Gulf of Mexico reduced the mean rainfall rate in India by about 50%. Such results are disturbing since the Gulf of Mexico (a proposed site for deployment of large numbers of OTPP's) is also the source region for most of the rainfall in the mid-western United States.

Investigation of changes induced in the three-dimensional, time-dependent state of the atmosphere requires a three-dimensional, time-dependent model. However, studies to assess the effect of OTPP operation on the local time-averaged state of the atmosphere can be accomplished with a one-dimensional, steady model. Such a model has been constructed for the special case of cloud-free conditions and these studies are in progress. The remainder of this report will describe the model, some preliminary results, and plans for future work.

Section 2

DESCRIPTION OF THE MODEL

2.1 BASIC MODEL EQUATIONS

Consider a region above the tropical ocean with an area large enough to encompass the sea surface temperature anomaly produced by several OTPP's yet small enough to be regarded as a small fraction of the atmosphere's general circulation system. Then, in the absence of clouds, the equations for conservation of momentum, moisture, and thermodynamic energy averaged horizontally in the region can be written

$$\frac{\partial u}{\partial t} = - \dot{\sigma} \frac{\partial u}{\partial \sigma} + f(v-v_g) - \frac{g}{p_*} \frac{\partial \tau_x}{\partial \sigma} \quad , \tag{1}$$

$$\frac{\partial v}{\partial t} = - \dot{\sigma} \frac{\partial v}{\partial \sigma} - f(u-u_g) - \frac{g}{p_*} \frac{\partial \tau_y}{\partial \sigma} \quad , \tag{2}$$

$$\frac{\partial q}{\partial t} = - \dot{\sigma} \frac{\partial q}{\partial \sigma} - \left[u \frac{\partial q}{\partial x} + v \frac{\partial q}{\partial y} \right] - \frac{g}{p_*} \frac{\partial Q}{\partial \sigma} \quad , \tag{3}$$

$$\frac{\partial T}{\partial t} = - \dot{\sigma} \frac{\partial T}{\partial \sigma} - \left[u \frac{\partial T}{\partial x} + v \frac{\partial T}{\partial y} \right] + \frac{RT_v}{c_p} \frac{\dot{\sigma}}{\sigma}$$

$$- \frac{g}{c_p p_*} \left[\frac{\partial F_S^*}{\partial \sigma} + \frac{\partial F_L^*}{\partial \sigma} \right] - \frac{g\sigma^{R/c_p}}{c_p p_*} \frac{\partial H}{\partial \sigma} \quad , \tag{4}$$

where

$$\sigma = p/p_*$$

has been used as the vertical coordinate. All the symbols are defined in the Appendix and most of the notation is standard. The first terms on the right-hand sides of (1) - (4) represent

the effect of advection by the average vertical motion in the region while the second terms on the right of (3) and (4) represent the effect of horizontal advection of moisture and temperature respectively. The treatment of the horizontal moisture and temperature advection will be discussed in Section 2.4. Note that the Rossby number of the flow is assumed $<<1$, which allows neglect of the horizontal advection terms in equations (1) and (2). The second terms on the right-hand sides of equations (1) and (2) represent the Coriolis force and the horizontal pressure gradient. The third term on the right of equation (4) represents compressional heating while the fourth term is the net radiational heating. The last terms on the right-hand sides of equations (1) to (4) represent the divergence of the vertical turbulent fluxes of E-W momentum, N-S momentum, moisture, and heat respectively.

2.2 TURBULENCE PARAMETERIZATION

Following many others, we divide the planetary boundary layer into two parts:

- a surface or "constant flux" layer, with a thickness of order 20m, in which the turbulent fluxes of momentum, moisture, and heat depart little from their surface values, and
- an overlying Ekman layer in which the fluxes generally decrease with height.

2.2.1 The Surface Layer

Under steady, horizontally homogeneous conditions, Monin-Obukhov similarity theory predicts that properly scaled vertical derivatives of wind speed, moisture, and temperature will be universal functions of z_1/L in the surface layer, where z_1 is the height above the surface and L is the Monin-Obukhov length. We impose the value $z_1 = 20$ m (the height of the first mesh-point in our representation.) The length L is negative in unstable cases, as described below. The surface eddy fluxes are then related to the wind speed, temperature and humidity at z_1, according to the "profile method" (Busch, 1977), by the following equations:

$$(\tau_o/\rho_a)^{\frac{1}{2}} = u_* = \frac{\kappa(U - U_o)}{\ln(z_1/z_o) - \psi_m(z_1/L)} \quad , \tag{5}$$

$$H_o = \frac{c_p \kappa u_* (T - T_o)}{\ln(z_1/z_o) - \psi_\theta(z_1/L)} \quad , \tag{6}$$

$$Q_o = \frac{\kappa u_* (q - q_o)}{\ln(z_1/z_o) - \psi_q(z_1/L)} \quad . \tag{7}$$

Here

$$\psi_\alpha = \int_0^{z_1/L} \{1 - \phi_\alpha(\zeta)\}\frac{\partial \zeta}{\zeta} \quad , \text{ for } \alpha = m,\theta,q, \tag{8}$$

where ϕ_m, ϕ_θ, and ϕ_q are non-dimensional gradients of wind, speed, temperature, and humidity respectively. Equations (6) - (8) have been used recently by Hsu (1974), Pond, et. al. (1974), Dunckel, et. al. (1974), and several others. The forms of the ϕ_α functions have recently been reviewed by Högstrom (1974) and it is generally accepted that most

atmospheric data are well represented by

$$\phi_m(\zeta) = \begin{cases} 1 + 5\zeta & \text{for } \zeta \geq 0 \\ (1 - 15\zeta)^{-\frac{1}{4}} & \text{for } \zeta < 0 \end{cases} \tag{9}$$

$$\phi_\theta = \phi_q = \begin{cases} 1 + 6\zeta & \text{for } \zeta \geq 0 \\ (1 - 9\zeta)^{-\frac{1}{2}} & \text{for } \zeta < 0 \end{cases} \tag{10}$$

which are the forms used in the model. The Monin-Obukhov length is calculated from

$$L = \frac{\rho_a u_*^3}{\kappa g(H_o/c_p T + 0.6Q_o)} \tag{11}$$

and is negative when the surface layer is hydrostatically unstable (see Kraus, 1972). Following Clarke (1970) and others, we assume

$$z_o = \max\,(0.032\ u_*^2/g\ ,\ z_{min}) \quad , \tag{12}$$

where z_{min} is 0.0015 cm.

The sea surface temperature provides the lower boundary condition for T and the specific humidity at the lower boundary is set equal to 0.98 times the saturation value at the sea surface temperature (to account for the effect of salt on the vapor pressure of water, see Roll, 1971). The wind velocity at the sea surface is set equal to the surface drift velocity, which is assumed to be in the direction of the geostrophic wind at the top of the Ekman layer and have a magnitude of

$$U_o = U_g\ (\rho_a/\rho_w)(\nu_a/\nu_w)^{\frac{1}{2}}$$

$$\sim U_g/200$$

(see Kraus, 1972). Equations (5) - (12) are solved iteratively at each time step in the numerical representation which we have adopted.

2.2.2 The Ekman Layer

The vertical eddy fluxes of momentum, heat, and moisture, in the Ekman layer are calculated from

$$\tau_x = - \frac{\rho^2 g}{p_*} K \frac{\partial u}{\partial \sigma} \quad ,$$

$$\tau_y = - \frac{\rho^2 g}{p_*} K \frac{\partial v}{\partial \sigma} \quad ,$$

$$H = - \frac{\rho^2 g c_p}{p_*} K \frac{\partial \theta}{\partial \sigma} \quad ,$$

$$Q = - \frac{\rho^2 g}{p_*} K \frac{\partial q}{\partial \sigma} \quad ,$$

$$K = \ell^2 \left| \frac{\partial U}{\partial z} \right| \quad ,$$

$$\theta = T \sigma^{-R/c_p} \quad ,$$

$$\rho = \frac{\sigma p_*}{R T_v} \quad ,$$

and the virtual temperature T_v is

$$T_v = T (1 + 0.61q)$$

Following Clarke (1970), the mixing length, ℓ, is specified as a function of z in a manner that depends on the sign of L. For negative L we define a "convection depth" height z_{cd} above which the Richardson number

$$Ri = N^2 / \left\{ (\partial u/\partial z)^2 + (\partial v/\partial z)^2 \right\}$$

is greater than unity. Here N is the usual Brunt-Vaisala frequency.

Then

$$\ell = \kappa z (1 - 15\, z/L)^{0.275} \quad , \quad \text{for } z < 0.3 z_{cd} \quad ,$$

$$\ell = \ell_o = 30 \text{ m} \quad , \quad \text{for } z > z_{cd} \quad ,$$

and ℓ is obtained by linear interpolation in the intervening range. For positive L, we define the mixing length as

$$\ell = \min \left\{ \kappa z (1 + 5z/L)^{-1} \, , \, \ell_o \right\} \quad , \quad \text{for } z < L \, ,$$

$$\ell = \min \left\{ \kappa z/6 \, , \, \ell_o \right\} \quad , \quad \text{for } z > L \, ,$$

where ℓ_o is again 30 m.

This treatment of the vertical diffusion coefficient has been used recently by Physick (1976) in a two-dimensional model of the sea breeze.

2.3 RADIATIVE TRANSFER EQUATIONS

The long-wave radiation equations used in our model are basically due to Danard (1969). For a cloud-free atmosphere, the zero approximation transparency yields an upward energy flux of $\varepsilon_o B_o T^4$. The infrared emissivity ε_o of the sea surface is taken as 0.97. The first approximation to the net downward long-wave radiation flux at a particular level is then

$$F_L^* = - \varepsilon_o B T_o^4 + \int_{\text{above}} B T^4 d\varepsilon$$

$$+ \int_{\text{below}} (\varepsilon_o B T_o^4 - B T^4) d\varepsilon .$$

Here $d\varepsilon$ is the emissivity and absorptivity of the layer between the level where the temperature is T and the level in question. The layers above add downward radiation according to their temperature, while the layers below absorb some of the upward radiation, and also emit new upward radiation according to their temperature. By definition, $d\varepsilon$ is given by

$$d\varepsilon = \varepsilon'(w)\, dw$$

where

$$dw = q\, (p/p_r)^{0.85} (T_r/T)^{0.5} (p_*/g)\, d\sigma$$

is the "precipitable water vapor" in the layer $d\sigma$ and ε' is the proportionality derivative. We approximate ε' by adapting Elsasser's (1960) experimental curve for the flux emissivity of pure water vapor.

The incoming short-wave radiation flux is $S_o \cos \alpha$, where S_o is the solar constant and α is the solar zenith angle. This flux is divided into two parts, following Arakawa, Katayama and Mintz (1968). The first part (blue, with wavelength smaller than about 0.9 μ) experiences significant Rayleigh scattering, but no absorption, while the second part (red, with larger wavelengths) experiences significant absorption but no scattering. The net downward short-wave radiation flux distribution at a particular level is taken in this model as

$$F_S^* = S_o \cos \alpha \left[0.651(1 - a_o)/(1 - a_o a_s) + 0.349\{1 - 0.03(w^* \sec \alpha)^{0.303}\} \right]$$

where w^* is the integral of the precipitable water vapor from the level in question to the top of the atmosphere, a_s is the albedo of the sea surface, taken as 0.065, and

$$a_o = 0.085 - 0.245 \log \left(\frac{p_*}{p_T} \cos \alpha \right)$$

where p_T is the pressure at the top of the model.

The solar zenith angle α is a function of the time of day, for each latitude ϕ and solar declination angle δ from the equatorial plane. The above expression for the downward flux is therefore integrated over the daylight hours to obtain the diurnal average flux distribution, as a function of ϕ and δ.

2.4 TREATMENT OF HORIZONTAL MOISTURE AND TEMPERATURE ADVECTION

The horizontal advection of moisture averaged across the model domain is parameterized by

$$u \frac{\partial q}{\partial x} + v \frac{\partial q}{\partial y} = \frac{U (q - q_{us})}{d}$$

where q_{us} is a specified function of altitude and is considered to be the specific humidity at some distance of order d upstream from the center of the region being modeled and U is the wind speed at the level in question. Hence, with respect to moisture advection, the model can be thought of as representing one horizontal grid point of a general circulation model with the vertical moisture profile held constant at the grid points upstream and the lateral advection of moisture computed with an upstream difference. In the context of the present study, q_{us} can be identified with the specific humidity distribution just upstream of the OTPP-generated sea surface temperature anomaly.

The horizontal advection of temperature averaged across the model domain follows from the thermal wind equation in σ coordinates which relates the horizontal gradient of temperature to the geostrophic wind (which is an imposed quantity in our model). Thus, for the case of flat surface topography, we have

$$u \frac{\partial T}{\partial x} + v \frac{\partial T}{\partial y} = \frac{f\sigma}{R} \left\{ u \left[\frac{v_{go}}{T_o} \frac{\partial T}{\partial \sigma} - \frac{\partial v_g}{\partial \sigma} \right] + v \left[\frac{\partial u_g}{\partial \sigma} - \frac{u_{go}}{T_o} \frac{\partial T}{\partial \sigma} \right] \right\}$$

with all the symbols defined in the Appendix.

2.5 GRID AND FINITE DIFFERENCE SCHEME

In order to resolve the surface layer without demanding unnecessary core storage, a vertically stretched grid is employed with the stretching function given by

$$\sigma_s = 1 - c_1 s^2 - c_2 s \quad , \tag{13}$$

with

$$c_1 = 0.001982$$

and

$$c_2 = 0.00036 \quad .$$

Equations (1) - (4) are solved at sigma levels defined by setting $s = 1, 2, 3, .., 20$ in (13) while the eddy diffusion coefficient is calculated at levels defined by $s = 3/2, 5/2, 7/2, .., 39/2$. This choice of parameters places the first grid point at approximately 20 m above the sea surface and the last grid point at about tropopause level.

The numerical scheme is forward in time with the eddy flux terms in (1) - (4) treated implicitly. The implicit treatment allows a much longer time step (typically 5-10 min) than would otherwise be possible.

Section 3

DESCRIPTION OF THE EXPERIMENTS

Values for the parameters listed in Table 1 (which are considered to be averaged horizontally across the model domain and in time over a period of about one month) are imposed, the sea surface temperature is specified, and (1) - (4) are integrated to a steady state from arbitrary initial conditions. The resulting solutions represent the mean state of the atmosphere averaged in time, and space as above. Then, with the same values for the imposed paramaters in Table 1, the model is integrated to other steady states corresponding to various sea, surface temperature perturbations, with the resulting differences in the thermodynamic characteristics of the atmosphere being the quantities of interest.

Three experiments are performed with the sea surface temperature specified as below:

Experiment	Sea Surface Temperature
1	302.0
2	301.5
3	301.0

These temperatures are in the range characteristic of the summertime tropical ocean.

Note that these experiments are of a very preliminary nature and serve primarily to illustrate the basic capabilities of this very simple model. In future studies, specific seasons and geographical locations will be investigated. In these cases, the parameters in Table 1 will have to be chosen very carefully from climatological data rather than specified in a simple fashion as is done here. In addition, the present model lacks a parameterization for clouds and rainfall. These effects are obviously fundamental in modeling the atmosphere in certain regions and during certain periods and must therefore be incorporated into later versions of the model.

Table 1

Imposed Parameters For All Three Experiments

Parameter	Symbol	Value
E-W component of geostrophic wind	u_g	10 m s^{-1}
N-S component of geostrophic wind	v_g	0
specific humidity at distance d upstream	q_{us}	see Fig. 1
length scale for lateral moisture advection	d	300 km
surface pressure	p_*	1000 mb
vertical motion in σ coordinate system	$\dot{\sigma}$	see Fig. 1
specific humidity at model top	q_t	0.09 g kg^{-1}
temperature at model top	T_t	$220^{\circ}K$
E-W component of wind at model top	u_t	10 m s^{-1}
N-S component of wind at model top	v_t	0
latitude	ϕ	25°
declination angle of sun	δ	20°

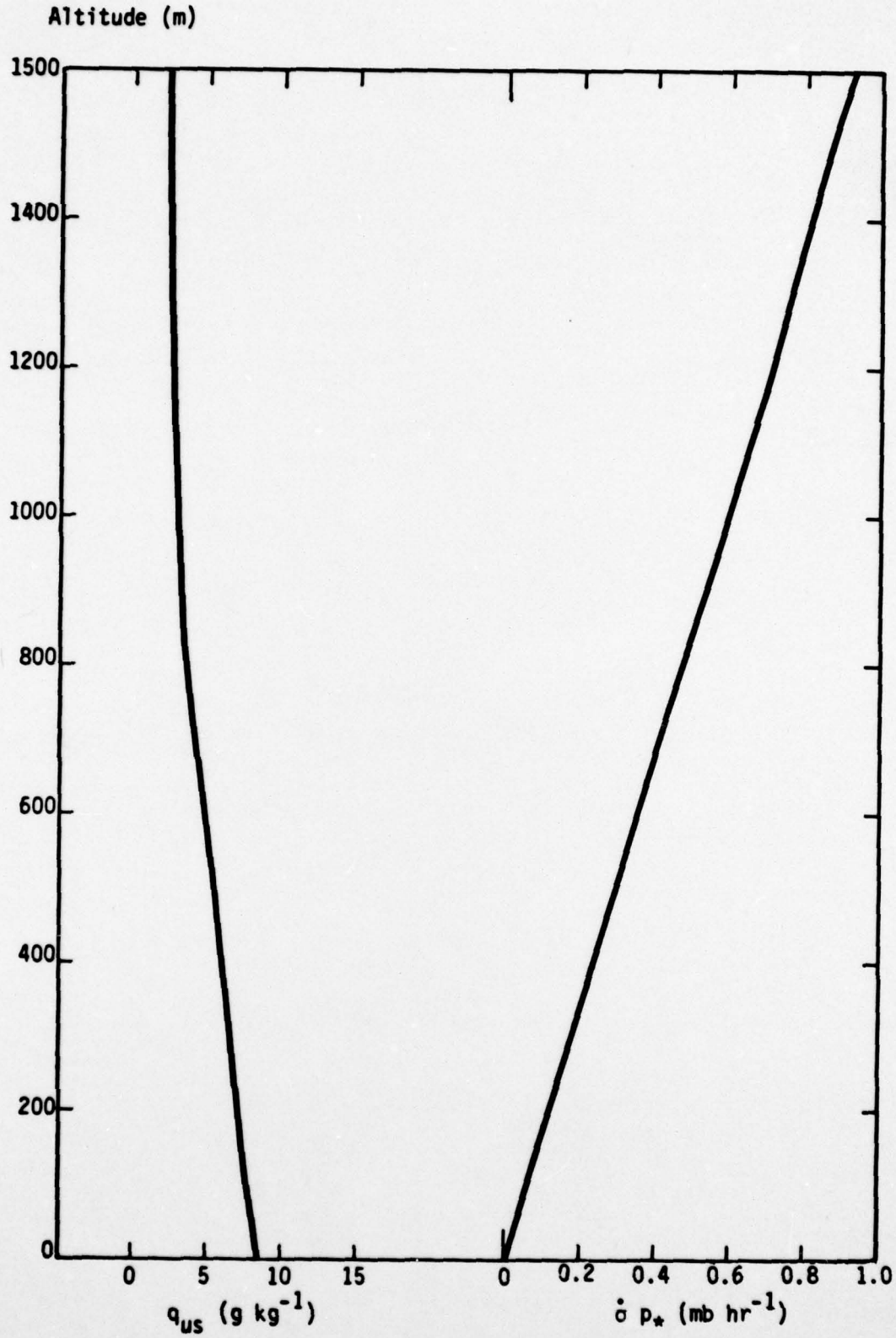

Figure 1. Prescribed profiles of the upstream humidity q_{us} and the vertical motion $\dot{\sigma}$ p_* in the lowest 1500 m, for all three experiments.

Section 4

RESULTS

Figure 2 shows vertical profiles of potential temperature and specific humidity in the lowest 1500 m of the atmosphere for the steady state attained in experiment 1. Note the presence of (a) the surface layer of thickness 20 m in which potential temperature and specific humidity decrease rapidly with height and (b) the Ekman layer of thickness 400 m in which potential temperature and specific humidity vary almost linearly and show only a slight decrease with height. The Ekman layer is topped by a stable layer in which the specific humidity decreases, first rapidly and then gradually, with height. These results represent a reasonable thermodynamic state for the cloud-free marine atmosphere.

Figure 3 shows vertical profiles of u and v for the steady state of Experiment 1. Note the large value of wind shear in the surface layer and the clockwise rotation of the wind vector with height in the Ekman layer, both of which are expected results.

The vertical profiles of u and v for Experiments 2 and 3 are essentially the same as in Experiment 1. However, the lowest 500 m in Experiment 2 is, on the average, 0.4°C cooler and 0.3 g kg^{-1} dryer than Experiment 1, while in Experiment 3 this layer is 0.8°C cooler and 0.6 g kg^{-1} dryer than Experiment 1. Hence, as expected, lower sea surface temperatures produce a cooler and dryer marine boundary layer. Furthermore, for the range of temperature perturbations considered, the decrease in the average temperature and moisture in the lower atmosphere is a linear function of the sea surface temperature.

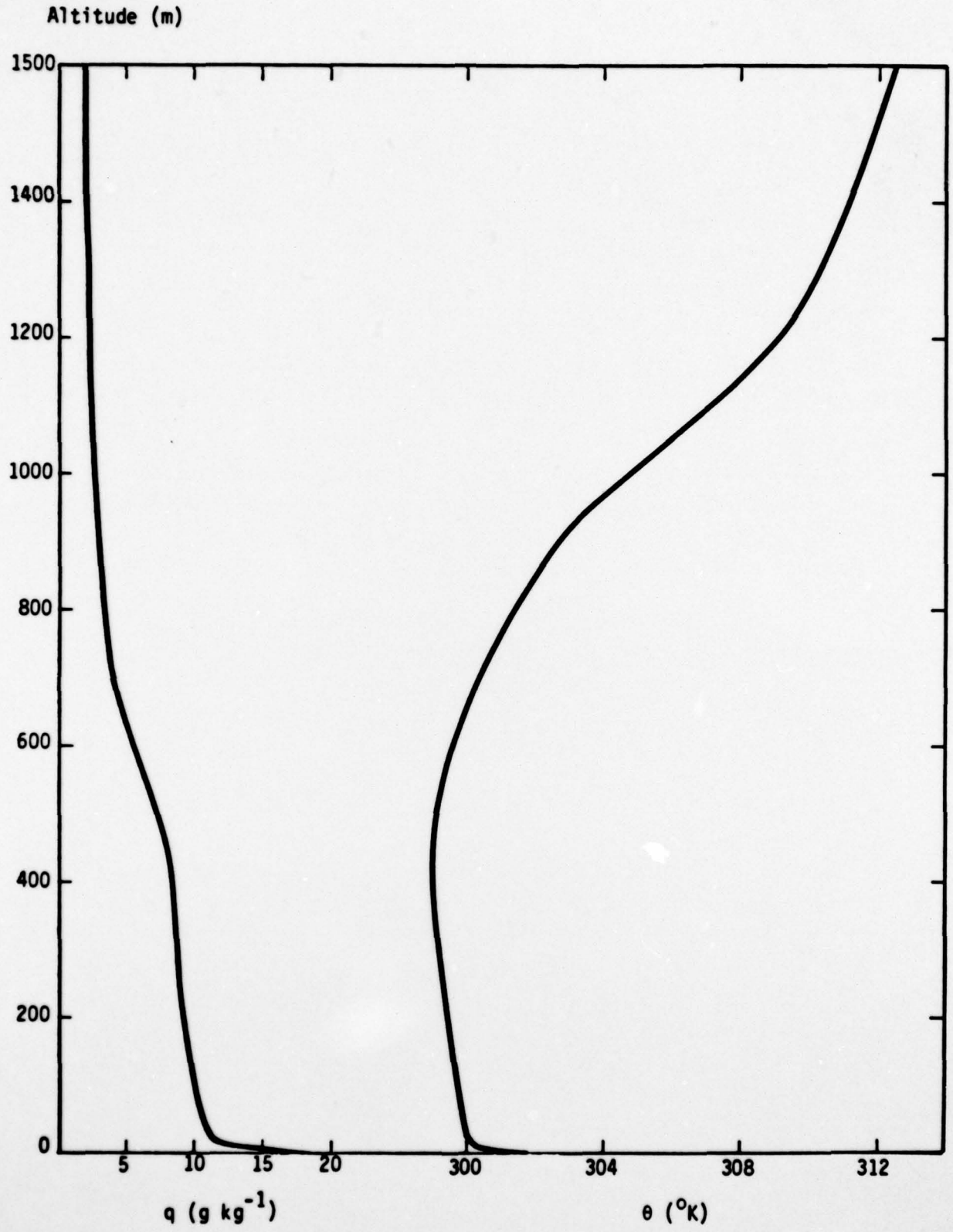

Figure 2. Specific Humidity and Potential Temperature in the Lowest 1500 m for the Steady State Attained in Experiment 1.

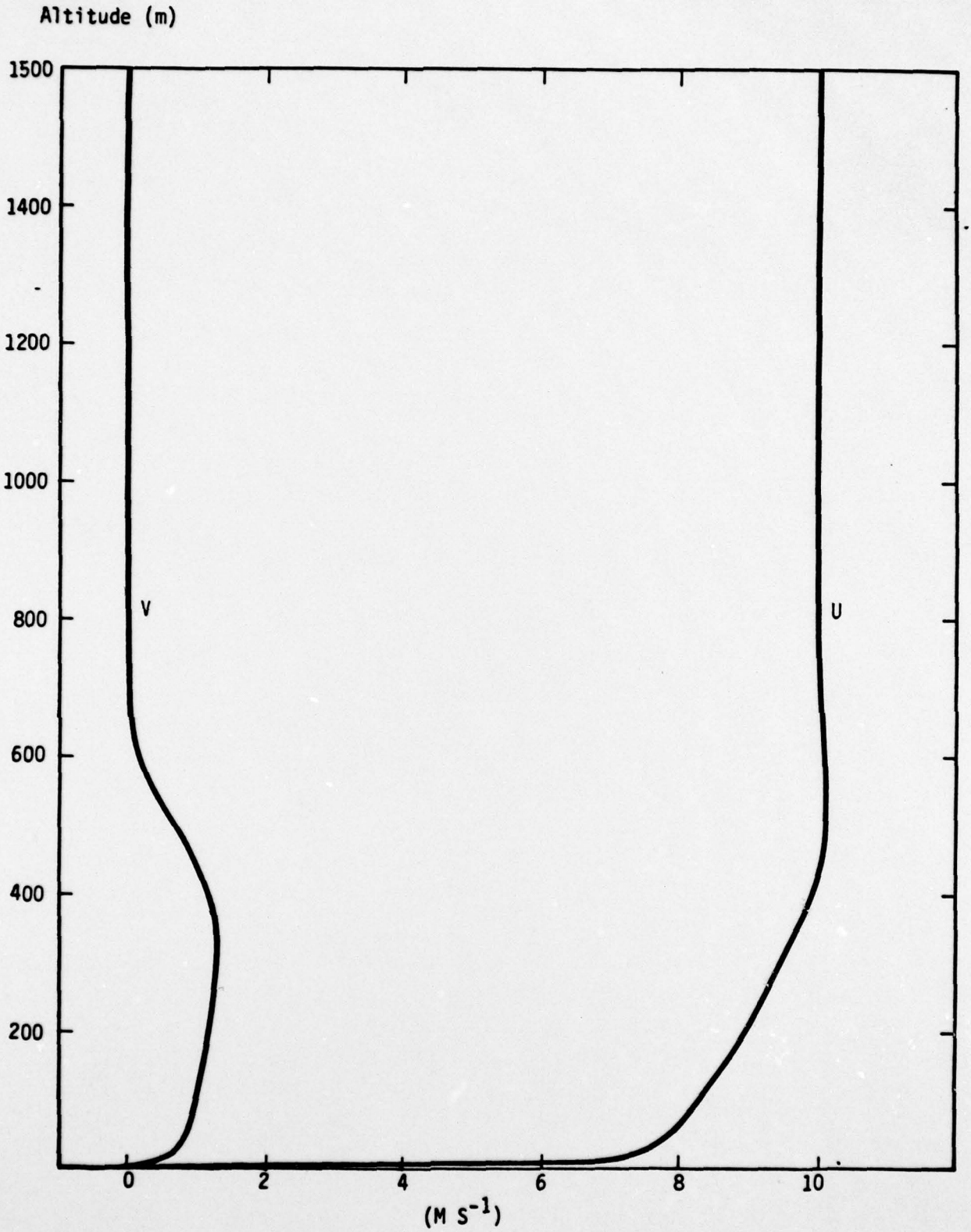

Figure 3. N-S and E-W Components of Wind Velocity in the Lowest 1500 m for the Steady State Attained in Experiment 1.

Table 2 gives values for the surface fluxes of latent heat, sensible heat, long-wave radiation, and short-wave radiation for all three experiments. The total surface heat balance, E_o, for Experiment 1 indicates a net heating rate for the upper ocean of 102 cal cm^{-2} day^{-1}. The net heating rates for Experiments 2 and 3 are 118 and 133 cal cm^{-2} day^{-1} respectively. Hence, the model predicts a linear variation of E_o with the sea surface temperature for perturbations of 1^oC or less. Furthermore, we find dE_o/dT_o = 31 cal cm^{-2} day^{-1} $^oC^{-1}$ which is about half the value estimated by Bathen et al. (1976) for a proposed OTPP site at Keahole Point, Hawaii, and about one-third the value estimated by Piacsek et al. (1976) for a proposed site off the southeast coast of Puerto Rico.

Both Piacsek et. al. (1976) and Bathen et al. (1976) used bulk aerodynamic formulations and local meteorological data to estimate the surface fluxes, and were forced to make certain arbitrary assumptions about the atmosphere's adjustment to the sea surface temperature perturbations. By modeling the atmosphere and explicitly predicting its adjustment to the sea surface temperature perturbation, we feel a more reliable determination of dE_o/dT_o can be obtained.

Table 2

Variation of the Surface Heat
Flux with the Sea Surface Temperature

Experiment	1	2	3
Sea surface temperature	302.0°K	301.5°K	301.0°K
Net solar radiation	920	920	920
Net infrared radiation	-449	-446	-444
Latent heat flux	-318	-307	-296
Sensible heat flux	-51	- 49	-47
Net surface heat flux	102	118	133

(Units for fluxes are cal cm^{-2} day^{-1}. Positive flux indicates flow of heat from air to water.)

Section 5

SUMMARY AND CONCLUSIONS

A one-dimensional numerical model has been constructed and used to investigate the effect of sea surface temperature perturbations generated by Ocean Thermal Power Plants on the thermodynamic structure of the cloud-free marine atmosphere. Conservation equations for momentum, moisture, and heat are solved on a vertically stretched grid extending from the sea surface to tropopause level. Long and short wave radiation, horizontal and vertical advection of heat and moisture by the large scale flow and vertical eddy fluxes of momentum, moisture, and heat are included. The vertical eddy fluxes are determined from Monin-Obukhov similarity theory for the surface layer, while in the remainder of the planetary boundary layer, a semi-empirical mixing length formulation is used.

Appropriately averaged values of the geostrophic wind and the large scale vertical motion field are imposed along with boundary conditions on the prognostic variables, and the model is integrated to a steady state. Then, for small changes in the sea surface temperature but with all other imposed parameters remaining the same, other steady states are determined with the resulting differences in the thermodynamic characteristics of the atmosphere being the quantities of interest.

It is found that for sea surface temperature perturbations of $1^{\circ}C$ or less, the average temperature and moisture in the marine boundary layer vary almost linearly with the sea surface temperature with slopes of 0.8 $^{\circ}C/^{\circ}C$ and 0.6 g $kg^{-1}/^{\circ}C$ respectively. The total heat flux at the sea surface is also found to vary linearly with the sea surface temperature in the range with a slope of 31 cal cm^{-2} $day^{-1}/^{\circ}C$.

Although these preliminary results indicate that OTPP operation will induce only a very minor change in the thermodynamic structure of the marine atmosphere, it must be reemphasized that the effect of cumulus clouds is ignored in the model. Hence, the predicted changes in the atmosphere's state for various sea surface temperature perturbations apply only to cloud-free conditions unless the assumption is made that the characteristics of the overlying cumulus cloud ensemble are unaffected by the OTPP-generated sea surface temperature anomaly. However, this is probably not a good assumption. For example, the observations reported by Malkus (1957) suggest that trade wind cumuli respond to sea surface temperature anomalies as small as 0.1 - 0.3°C. Therefore changes induced in the thermodynamic structure of the sub-cloud layer by OTPP operation are likely to affect the cumulus clouds which, in turn, affect the thermodynamics of the sub-cloud layer themselves (Ogura and Cho, 1973; Esbensen, 1975). Thus, feedback effects are possible that might amplify the surface flux perturbations resulting from OTPP operation.

Furthermore, because of the tendency for equivalent potential temperature to be conserved in moist convection and the exponential dependence of saturation specific humidity on temperature, small changes in the temperature at cloud base yield much larger changes in the temperature at cloud top. Therefore, to achieve a better prediction of the atmosphere's adjustment to OTPP-generated sea surface temperature anomalies, the model should be extended to include a parameterization of the thermodynamic effect of cumulus clouds. The cumulus parameterization scheme of Arakawa and Schubert (1974) provides the only closed theory for the mutual interaction of a cumulus cloud ensemble with the large-scale environment and is now being incorporated into the model.

Appendix

List of Symbols

a_s	albedo of sea surface
B	Stefan-Boltzmann constant
c_p	specific heat at constant pressure for air
c_1, c_2	stretched-grid parameters
d	horizontal length scale for calculation of lateral moisture advection
E_o	net heat flux at sea surface (positive downward)
F_L^*, F_S^*	net downward flux of long-wave radiation, short-wave radiation
f	Coriolis parameter
g	acceleration of gravity
H_o, H	vertical eddy flux of sensible heat in surface layer, Ekman layer
K	vertical diffusion coefficient for momentum, moisture, and heat
ℓ	mixing length
L	Monin-Obukhov length
N	Brunt-Vaisala frequency
p, p_*, p_r, p_T	pressure, surface, pressure, reference pressure, pressure at model top
Q_o, Q	vertical eddy flux of moisture in surface layer, Ekman layer
q, q_o	specific humidity, specific humidity at sea surface
q_{us}	specific humidity at distance d upstream from the center of the model domain

R	gas constant for dry air
S_o	solar constant
T, T_o	temperature, sea surface temperature
T_v, Tr	virtual temperature, reference temperature
U, U_o	wind speed, wind speed at sea surface
U_g	geostrophic wind at top of Ekman layer, $\left(u_g^2 + v_g^2\right)^{\frac{1}{2}}$
u_*	surface friction velocity $(\tau_o/\rho_a)^{\frac{1}{2}}$
u, u_g, u_{go}	E-W component of wind, E-W component of geostrophic wind, E-W component of geostrophic wind at sea surface
v, v_g, v_{go}	N-S component of wind, N-S component of geostrophic wind, N-S component of geostrophic wind at sea surface
w	precipitable water vapor
w_o, w_t	precipitable water vapor at sea surface, model top
z	height above sea surface
z_{cd}	height at which Richardson number equals 1
z_o	surface roughness length
z_1	height of first grid point above sea surface
κ	von Karman's constant
ρ	density of air
ρ_a, ρ_w	reference density for air, water
ν_a, ν_w	molecular viscosity of air, water
ϕ	latitude
$\phi_m, \phi_\theta, \phi_q$	non-dimensional gradients of wind speed, temperature, and humidity in the surface layer
τ_o	wind stress at sea surface

τ_x, τ_y	vertical flux of E-W momentum, N-S momentum (i.e., components of turbulent shear stress)
σ	vertical coordinate, p/p_*
$\dot{\sigma}$	vertical motion in σ coordinate system, $d\sigma/dt$
θ	potential temperature, $T\sigma^{-R/c_p}$
ε_o	infrared emissivity of sea surface
ε'	derivative of infrared emissivity with respect to precipitable water vapor
α	solar zenith angle

References

Arakawa, A., A. Katayama, and Y. Mintz, 1968. Numerical simulation of the general circulation of the atmosphere. Proc. WMO (IUGG Symp. National Weather Prediction), Tokyo.

Arakawa, A., and W. H. Schubert, 1974. Interaction of a cumulus cloud ensemble with the large-scale environment, Part I. J. Atmos. Sci., 31, 674-701.

Bathen, K. H., et al., 1976. A further evaluation of the oceanographic conditions off Keahole Point, Hawaii, and the environmental impact of nearshore OTEC plants on subtropical Hawaiian waters. Final report, Department of Ocean Engineering, Univ. of Hawaii.

Busch, N. E., 1977. Fluxes in the surface boundary layer over the sea. Chapt. 6, Modelling and Prediction of the Upper Layers of the Ocean, Pergamon Press.

Clarke, R. H., 1970. Recommended methods for the treatment of the boundary layer in numerical models. Aust. Meteor. Mag., 18, 51-73.

Danard, M. B., 1969. A simple method of including longwave radiation in a tropospheric numerical prediction model. Mon. Wea. Rev., 97, 77-85.

Dunckel, M., L. Hasse, L. Krügermeyer, D. Schriever, and J. Wucknitz, 1974. Turbulent fluxes of momentum, heat and water vapor in the atmospheric surface layer at sea during ATEX. Boundary-Layer Meteorol., 6, 81-106.

Esbensen, S., 1975. An analysis of subcloud-layer heat and moisture budgets in the western Atlantic trades. J. Atmos. Sci., 32, 1921-1933

Elsasser, W. M., 1960. Meteorol. Monographs 4 (23), 43 pp.

Hsu, S. A., 1974. On the log-linear wind profile and the relationship between shear stress and stability characteristics over the sea. Boundary-Layer Meteorol., 6, 509-514.

Hogstrom, U., 1974. A field study of the turbulent fluxes of heat, water vapour and momentum at a "typical" agricultural site. Quart. J. Roy. Meteorol. Soc., 100, 624-639.

Kraus, E. B., 1972. Atmosphere-Ocean Interaction, Clarendon Press, 275 pp.

Malkus, J. S., 1957. Trade cumulus cloud groups. Some observations suggesting a mechanism of their origin. Tellus, 9, 33-44.

Ogura, Y., and H. R. Cho, 1974. On the interaction between the subcloud and cloud layers in tropical regions. J. Atmos. Sci., 31, 1850-1859.

Physick, W., 1976. A numerical model of the sea-breeze phenomenon over a lake or gulf. J. Atmos. Sci., 33, 2107-2135.

Piacsek, S., P. Martin, J. Toomre, and G. Roberts, 1976. Recirculation and thermocline perturbations from ocean thermal power plants. NRL-GFD/OTEC 2-76, 25 pp.

Pond, S., D. B. Fissel, and C. A. Paulson, 1974. A note on bulk aerodynamic coefficients for sensible heat and moisture fluxes. Boundary-Layer Meteorol., 6, 333-339.

Roll, H. U., 1965. Physics of the Marine Atmosphere, Academic Press, 426 pp.

Shukla, J., 1975. Effect of Arabian Sea surface temperature anomaly on Indian summer monsoon: A numerical experiment with the GFDL model. J. Atmos. Sci., 32, 503-511.